

# Large-scale flow formation in ensembles of swimming bacteria: Theory

Igor S. Aranson<sup>1</sup>, Andrey Sokolov<sup>1,2</sup>, Raymond E. Goldstein<sup>3</sup>, and John O. Kessler<sup>3</sup>

<sup>1</sup>Argonne National Laboratory, 9700 South Cass Avenue, Argonne, Illinois, 60439

<sup>2</sup>Illinois Institute of Technology, 3101 South Dearborn Street, Chicago, IL60616

<sup>3</sup>Department of Physics, University of Arizona, Tucson, Arizona 85721, USA

(Dated: April 1, 2006)

We develop mathematical model of hydrodynamically-induced self-organization of concentrated ensembles of swimming bacteria *Bacillus Subtilis* in thin fluid film. Starting from elementary stochastic interaction rules between self-propelled objects, we derive a set of equations for the local concentration and orientation of swimmers, coupled to the Navier-Stokes Equation for the fluid. We demonstrate that this system exhibits formation of self-organized large-scale patterns with the typical scale determined by the density of bacteria.

PACS numbers: 87.16.-b, 05.65.+b, 47.55.+r

Recent experiments [4, 5, 8] demonstrated significance of self-induced hydrodynamic flows produced by flagella of swimming bacteria. The characteristic scale of these flows typically exceed by the order of magnitude the size of individual element. The large-scale collective flows emerging in dense ensembles swimming particles in confined geometries are important for a variety of fundamental and technological reasons, ranging from understanding of the onset of coherent motion in groups of locally interacting objects (flocks, schools, herds [10, 11]), to potential microfluidic and biomedical devices [6].

Despite significant knowledge accumulated in experiments, [4, 5, 8, 9, 13], the intrinsic mechanisms of self-organization were not well-understood. One of the most intriguing questions, the origin of nontrivial characteristic scale of large-scale flows and its dependence on system parameters, remains unanswered. Simplified direct simulations of ensemble of swimming particles, while clearly identifying the significance of pure hydrodynamic interaction [7], do not provide a clear answer on the mechanisms of scale selection and the nature of transition from random motion in low density system of swimmers to collective motion at higher densities. Various phenomenological models of organization of self-propelled particles [10–12] do not account for long-range hydrodynamic interactions and, therefore, have only limited applicability to the system under study.

Motivated by recent experiments on self-organization of swimming bacteria *Bacillus Subtilis* in two-dimensional fluid films [4], in this Letter we derive continuum model governing self-organization of ensembles of hydrodynamic self-propelled particles. The model is formulated in terms of two-dimensional stochastic Master equation for the probability density  $P(\mathbf{r}, \phi)$  finding a bacteria at certain orientation angle  $\phi$  at the position  $\mathbf{r}$  derived from microscopic interaction rules. The Master equation provides a link between microscopic scale (individual bacteria) and macroscopic scale (collective motion), which is described by the set of equations for local bacteria density and orientation. The macroscopic equations are

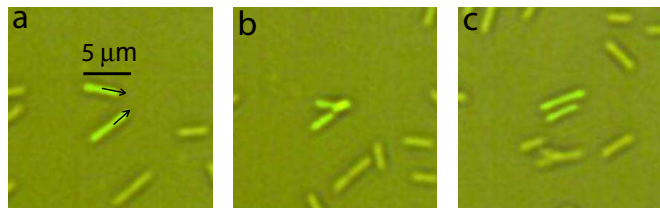


FIG. 1: Sequence of experimental images illustrating “inelastic collisions” between bacteria *Bacillus Subtilis*. Colliding bacteria (highlighted) swim from left to right: a) before the collision; b) collision; c) after collision. See Movie 1 in [18]

obtained by coarse-graining of the Master equation. The system is supplemented by the two-dimensional Navier-Stokes equation for the fluid flows with additional forcing term due to oriented bacteria swimming. The model reveals characteristic scale selection mechanism due to the deflection of swimming direction of the bacteria by the self-induced shear flow. The results are in qualitative agreement with the experiment [4].

*Master Equation.* We approximate bacteria by identical polar self-propelled rods of length  $l$  and diameter  $d_0$ . The model is derived from the following elementary interaction rules: (a) individual bacteria swim with the velocity  $v_0$  with respect to ambient fluid in the direction given by its unit orientation vector  $\mathbf{n} = (\cos \phi, \sin \phi)$ ; (b) in the case of collision of two bacteria with the angles  $\phi_{1,2}$  the pair continue to swim in the direction of average orientation  $\bar{\phi} = (\phi_1 + \phi_2)$ . We call this process, by analogy with physics of grains, fully inelastic collision. This assumption is justified by experimental observations, see Fig. 1. The underlying reason for the inelastic collisions between the bacteria lays in the dipole nature of the velocity field. We also assume that the bacteria experience rotational and translational diffusion, mostly due to tumbling and small-scale hydrodynamic flows. In addition, we include advection of bacteria by the fluid.

Using the analogy between motion of bacteria and the dynamics of inelastically colliding polar rods [1, 2], the

Master equation describing the evolution of probability  $P(\mathbf{r}, \phi)$ :

$$\begin{aligned} \partial_t P(\mathbf{r}, \phi) + \nabla \cdot ((v_0 \mathbf{n} + \mathbf{v})P(\mathbf{r}, \phi)) + \frac{1}{2} \Omega \partial_\phi P(\mathbf{r}, \phi) = D_r \partial_\phi^2 P(\mathbf{r}, \phi) + \partial_i D_{ij} \partial_j P(\mathbf{r}, \phi) + \int \int d\mathbf{r}_1 d\mathbf{r}_2 \int_{-\phi_0}^{\phi_0} dw \\ \times W(\mathbf{r}_1, \mathbf{r}_2) P(\mathbf{r}_1, \phi_1) P(\mathbf{r}_2, \phi_2) \left[ \delta \left( \frac{\mathbf{r}_1 + \mathbf{r}_2}{2} - \mathbf{r}, \frac{\phi_1 + \phi_2}{2} - \phi \right) - \delta(\mathbf{r}_2 - \mathbf{r}, \phi_2 - \phi) \right] \end{aligned} \quad (1)$$

The first two terms in the r.h.s. of (1) describe angular and translational diffusion of rods with the diffusion tensor  $D_{ij} = \frac{1}{D_r} (D_{\parallel} n_i n_j + D_{\perp} (\delta_{ij} - n_i n_j))$ .  $D_r, D_{\parallel}, D_{\perp}$  are known in polymer physics:  $D_{\parallel} = \frac{k_B T_e}{\xi_{\parallel}}, D_{\perp} = \frac{k_B T_e}{\xi_{\perp}}, D_r = \frac{4k_B T_e}{\xi_r}$  where  $\xi_{\parallel}, \xi_{\perp}, \xi_r$  are corresponding drag coefficients. For rod-like molecules,  $\xi_{\parallel} = 2\pi\eta_s l / \log(l/d_0)$ ;  $\xi_{\perp} = 2\xi_{\parallel}$ ;  $\xi_r \approx \pi\eta_s l^3 / 3 \log(l/d_0)$  where  $\eta_s$  is shear viscosity and  $T_e$  is effective temperature [14]. However, in contrast to polymer molecules, the effective temperature  $T_e$  is determined mostly by small-scale hydrodynamic flows and tumbling of bacteria, and can considerably exceed the thermodynamic temperature.

Terms  $\nabla \mathbf{v} P(\mathbf{r}, \phi) + \frac{1}{2} \Omega \partial_\phi P(\mathbf{r}, \phi)$  account for the advection of particles by hydrodynamic flow  $\mathbf{v}$  and rotation of the orientation vector in the shear flow with the vorticity

$$\Omega = \partial_y v_x - \partial_x v_y \quad (2)$$

The last term of Eq.(1) describes short-range binary interaction of rods. We assume that after the interaction, the two rods acquire the same orientation and the same spatial location in the middle of their original locations, consistent with experimental data on interaction of bacteria, see Fig. 1. Two  $\delta$ -functions in the collision integral describe ‘‘annihilation’’ of particle with the angle  $\phi_1$  and ‘‘creation’’ of particle with the angle  $(\phi_1 + \phi_2)/2$ . The interaction kernel  $W$  is localized in space (here we neglect anisotropy of the kernel essential for self-organization of microtubules [1, 2]). We assume for simplicity the following form:  $W = \frac{g}{b^2\pi} \exp \left[ -\frac{(\mathbf{r}_1 - \mathbf{r}_2)^2}{b^2} \right]$  with  $b \approx l = \text{const}$  and  $g = \text{const}$  is the interaction cross-section. This form implies that only nearby bacteria interact effectively.

We introduce the following *coarse-grained variables*: local density  $\rho(\mathbf{r}) = \int_{-\pi}^{\pi} P(\mathbf{r}, \phi) d\phi$  and local orientation vector  $\boldsymbol{\tau} = \langle \mathbf{n} \rangle = \int_{-\pi}^{\pi} \mathbf{n}(\mathbf{r}) P(\mathbf{r}, \phi) d\phi / 2\pi$ . These quantities are related to corresponding Fourier harmonics  $P_k = \langle e^{-ik\phi} \rangle$ . The zeroth harmonic  $P_0 = \rho / 2\pi = \text{const}$ , and the real and imaginary parts of  $P_1$  represent the components  $\tau_x = \langle \cos \phi \rangle, \tau_y = \langle \sin \phi \rangle$  of the average orientation vector  $\boldsymbol{\tau}$ . Spatially-homogeneous Eq. (refmaster3) exhibit onset of oriented state above critical density  $\rho_c = D_r / (4/\pi - 1) / g$  (see for detail [1]). New the threshold of the orientational instability Eq. (1) can be significantly simplified by means of standard bifurcation

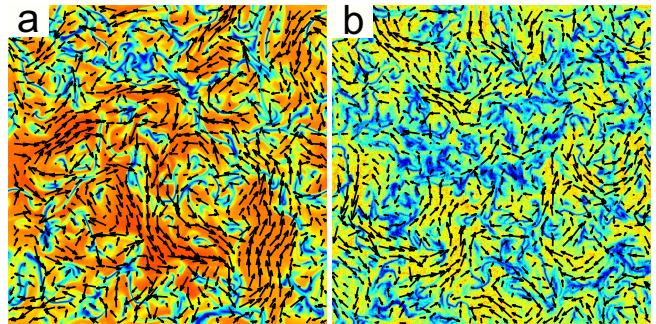


FIG. 2: Representative flow patterns obtained by solution of Eqs. (3),(4),(8) for  $\rho_0 = 3.8, D_0 = 50, \nu = 3 \dots$ . Red color corresponds to maximum of  $|\boldsymbol{\tau}|$ , and blue to minimum. Arrows depict the flow velocity  $\mathbf{v}$  field. See also Movie 2 [18]

analysis and the description can be reduced to the pair of coupled equations for  $\rho$  and  $\boldsymbol{\tau}$ . Since near the threshold  $P(\mathbf{r}, \phi)$  depends slowly on spacial variable  $\mathbf{r}$ , we perform Fourier expansion of Eq. (1) in  $\phi$  and truncate the series at  $|n| > 2$  and keep only leading terms in expansion on space gradients of  $P(\mathbf{r}, \phi)$ . Omitting calculations (see [1, 2]), rescaling space by  $l$ , and changing variables  $t \rightarrow D_r t, \rho \rightarrow g\rho / D_r$ , one obtains.

$$\partial_t \rho + \nabla \mathbf{v} \rho = D_0 \nabla^2 \rho - v_0 \pi \nabla \boldsymbol{\tau} \quad (3)$$

$$\begin{aligned} \partial_t \boldsymbol{\tau} + \mathbf{v} \nabla \boldsymbol{\tau} + \frac{1}{2} \Omega \times \boldsymbol{\tau} = (\epsilon \rho - 1) \boldsymbol{\tau} - A_0 |\boldsymbol{\tau}|^2 \boldsymbol{\tau} \\ + D_1 \nabla^2 \boldsymbol{\tau} + D_2 \nabla \nabla \cdot \boldsymbol{\tau} - \frac{v_0}{4\pi} \nabla \rho \end{aligned} \quad (4)$$

Eq. (3) describes advection of the bacteria by hydrodynamic velocity  $\mathbf{v}$  and diffusive spreading with the diffusion coefficient  $D_0$ . Here  $D_1 = (D_{\parallel} + D_{\perp}) / 2D_r l^2, D_2 = (D_{\parallel} - D_{\perp}) / 2D_r l^2$ . In the limit of small density  $\rho$  and for the case of pure thermal diffusion of particles the diffusion coefficients  $D_0 = (D_{\parallel} + D_{\perp}) / 2D_r l^2$ . However in our case this connection is not obvious, especially for larger densities due to diffusive-type contribution from the collision integral in Eq. (1). Since in experiments no significant density fluctuations were observed, we will treat  $D_0 \gg D_{1,2}$  as independent parameter in order to suppress density variations. In Eq. (4) the first term in

the r.h.s. describes the orientation instability,  $\epsilon = 0.276$ ,  $A_0 = 2.81$  for fully inelastic particles [1, 2]. The terms proportional to  $v_0$  are due to swimming of bacteria with respect to fluid.

For the hydrodynamic velocity  $\mathbf{v}$  we obtain the Navier-Stokes equation with forcing due to swimming of bacteria

$$\partial_t \mathbf{v} + \mathbf{v} \nabla \mathbf{v} = \nu \nabla^2 \mathbf{v} - \nabla p - \beta \mathbf{v} + \alpha \boldsymbol{\tau} \quad (5)$$

$$\nabla \mathbf{v} = 0 \quad (6)$$

where  $\nu$  is the viscosity,  $p$  is the pressure,  $\beta \mathbf{v}$  accounts for the damping due to friction with the walls,  $\alpha \boldsymbol{\tau}$  with  $\alpha \sim v_0$  models the forcing due to bacteria swimming. The damping  $\beta v$  is generated by the thin film viscoelasticity resulting in the partial slip condition for the velocity on the surface of the film. While our experiment, as well as of Ref. [5], are performed in the free-hanging film geometry, the surfactant accumulated on both surfaces of the fluid film play the role of semi-flexible walls resulting in nontrivial velocity profile across the film. The forcing term in Eq. (5) is different from that for the self-propelled particles proposed in Ref. [3], where the force is represented by the divergence of certain three-dimensional stress tensor  $\sigma_{ij}$ . However, integration of the stress tensor over the cross-section of the film produces similar terms  $\sim \tau$  due to the boundary effects.

In order to exclude pressure and satisfy continuity condition Eq. (6) we introduce stream function  $\phi$

$$v_x = \partial_y \phi, v_y = -\partial_x \phi, \quad \Omega = \nabla^2 \phi \quad (7)$$

Thus, from Eqs. (2,5) one obtains

$$\partial_t \Omega + \mathbf{v} \nabla \Omega = \nu \nabla^2 \Omega - \beta \Omega + \alpha (\partial_y \tau_x - \partial_x \tau_y) \quad (8)$$

Eqs. (9,8) and (7) form closed system. For the low Reynolds number flow the advection term  $\mathbf{v} \nabla \Omega$  can be neglected comparing to the viscosity term  $\nu \nabla^2 \Omega$ , but we keep it since similar term is included in Eq. (9). While the Reynolds number  $Re$  of individual bacteria is exceedingly small, for the collective flows  $Re$  of the order of one and, thus, the inertia effect are not negligible.

To simplify the analysis we consider constant density approximation  $\rho = \rho_0 = \text{const}$  valid for large bacterial diffusion  $D_0$ . Then Eq. (4) reduces to

$$\begin{aligned} \partial_t \boldsymbol{\tau} + \mathbf{v} \nabla \boldsymbol{\tau} + \frac{\Omega \times \boldsymbol{\tau}}{2} \\ = (\epsilon \rho - 1) \boldsymbol{\tau} - A_0 |\boldsymbol{\tau}|^2 \boldsymbol{\tau} + D_1 \nabla^2 \boldsymbol{\tau} + D_2 \nabla \nabla \cdot \boldsymbol{\tau} \end{aligned} \quad (9)$$

Eqs. (4, 8) have steady-state uniform solution corresponding to homogeneous stream of bacteria in a certain (e.g.  $x$ ) direction:  $\tau_x = \tau_0 = \sqrt{(\epsilon \rho - 1)/A_0} = \text{const}$ ,  $\tau_y = 0$ ,  $v_y = 0$ ,  $v_x = V = \alpha \tau_0 / \beta$ . To examine the stability, we represent perturbations in the form  $(\boldsymbol{\tau}, \Omega) \sim \exp[\lambda t + ikx]$ , where  $\lambda$  is the growthrate and  $k$  is the modulation waveguide. Linearized Eqs. (4, 8) are:

$$\lambda \tau_x = -ikV \tau_x - 2\tau_0^2 \tau_x - (D_1 + D_2) k^2 \tau_x \quad (10)$$

$$\lambda \tau_y = -ikV \tau_y - \frac{1}{2} \Omega \tau_0 - D_1 k^2 \tau_y \quad (11)$$

$$\lambda \Omega = -ikV \Omega - \nu k^2 \Omega - \beta \Omega - ik \alpha \tau_y \quad (12)$$

Equation for  $\tau_x$  splits off and we need to deal with only equations for  $\tau_y, \Omega$ . They yield the following expression for the growthrate  $\lambda$ :

$$\begin{aligned} \lambda_{1,2} = \frac{1}{2} \left( -(D_1 + \nu) k^2 - \beta - 2ikV \right. \\ \left. \pm \sqrt{((D_1 - \nu) k^2 - \beta)^2 - 2ik\tau_0 \alpha} \right) \quad (13) \end{aligned}$$

The instability occurs if the parameter  $\alpha \tau_0$  is greater than some critical value. Onset of instability can be obtained in the limit  $k \rightarrow 0$ . Expansion yields

$$Re \lambda = \left( \frac{\alpha^2 \tau_0^2}{\beta^3} - D_1 \right) k^2 + O(k^4) \quad (14)$$

Eq. (14) produces long-wave instability for  $\alpha^2 \tau_0^2 > \beta^3 D_1$ . Using that  $V = \alpha \tau_0 / \beta$  is the collective steady-state swimming velocity, we obtain simple condition  $V > V_d$ , where  $V_d = \sqrt{\beta D_1}$  is the ‘‘decoherence’’ velocity. Since  $\beta \sim \nu / d^2$ ,  $d$  is the film thickness, we obtain  $V_d = \sqrt{\nu D_1} / d$ . The selected wavenumber  $k_m$  can be obtained in the limit of large collective swimming speed  $V$ . Expanding Eq. (13) for  $\alpha \tau_0 \gg 1$  we obtain

$$Re(\lambda) \approx \frac{1}{2} \left( -(D_1 + \nu) k^2 - \beta + \sqrt{|k| \tau_0 \alpha} \right) + \dots \quad (15)$$

Then from Eq. (15) one derives (for  $(D_1 + \nu) k^2 \gg \beta$ )

$$k_m^{3/2} = \frac{\sqrt{\tau_0 \alpha}}{4(D_1 + \nu)} \quad (16)$$

Since  $\alpha \sim \nu v_0 l / d$ ,  $l$  is the length of bacteria and  $d$  is the film thickness (here we used expression for the drag force  $F \sim \eta v_0 l$  and included the scaling of orientation  $\tau$  with the film thickness  $d$ ), and  $\tau_0 \sim \sqrt{\rho - \rho_c}$ ,  $\rho_c$  is the critical density of the orientation instability, we obtain

$$k_m \sim \left[ \frac{v_0 l (\rho - \rho_c)^{1/2}}{d \nu^2} \right]^{1/3} \quad (17)$$

Thus, the typical length scale of the instability  $\sim 1/k_m$  scales with the film thickness at the threshold as  $d^{1/3}$ , in qualitative agreement with the simulations of [7].

We conducted *numerical studies* of full system (3),(4), and (8). The calculations were performed in a rather large domain (up to  $200 \times 200$  bacteria sizes) and in the range of densities  $\rho$ , and in periodic boundary conditions. Typical flow pattern and  $|\boldsymbol{\tau}|$  distribution is shown in Fig. 2. Remarkably, the correlation over the entire

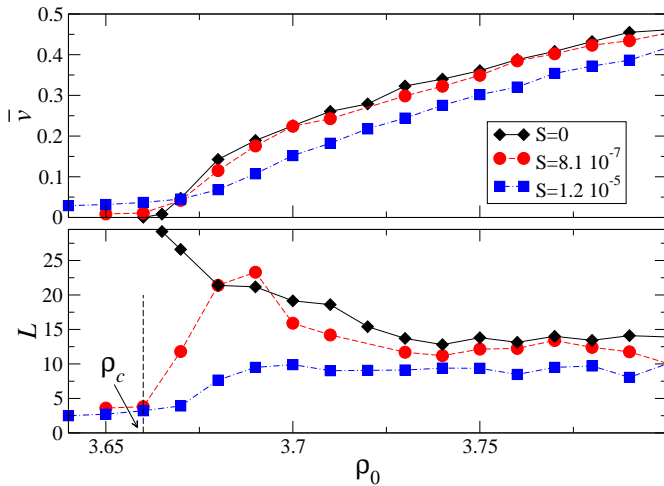


FIG. 3: Typical hydrodynamic velocity  $\bar{v}$  (upper panel) and velocity correlation length  $L$  vs density for three different level of noise  $S$ . for the following values of parameters: domain size  $200 \times 200$ ,  $v_0 = 0.2$ ,  $D_0 = 50$ ,  $\nu = 3$ ,

cell between the fields  $\boldsymbol{\tau}$  and  $\mathbf{v}$  happens to be close to zero, in agreement with experiment. However, there is always local correlation between  $\boldsymbol{\tau}$  and  $\mathbf{v}$  due functional coupling through Eq. (8).

The following quantities were evaluated in numerical studies: typical hydrodynamic velocity  $\bar{v} = \sqrt{\langle \mathbf{v}^2 \rangle - \langle \mathbf{v} \rangle^2}$ , and radial velocity correlation functions  $K(r)$ , defines as ( $\theta$  is a polar angle)

$$K(r) = \int_0^{2\pi} d\theta \langle \mathbf{v}(\mathbf{r}') \mathbf{v}(\mathbf{r} + \mathbf{r}') \rangle \quad (18)$$

The correlation length was extracted from  $K(r)$  by exponential fit  $K(r) \sim \exp(-x/L) + \text{const}$ . The results are comprised in Fig. 3. The overall picture of the transition bears strong feature of the second order phases transition: the typical velocity  $\bar{v} \sim \sqrt{\rho - \rho_c}$ , and the correlation length diverges at the critical density, consistent with the prediction of Eq. (16). The first order phase transition was found for a broad class of models of self-propelled particles Ref. [10]. However, the models considered in Ref. [10] do not include long-range effect of hydrodynamic interaction, which possibly could alter the type of transition.

In order to include effect of fluctuation, we added random force  $\zeta(x, y, t)$ ,  $\langle \zeta(x, y, t) \zeta^*(x', y', t') \rangle = 2S\delta(x - x')\delta(y - y')\delta(t - t')$ ,  $S$  is the noise strength, to the equation for orientation (4). Results of calculations for various noise strength shown in Fig. 3. As one sees, relatively small noise ( $S = 1.2 \times 10^{-7}$ ) smears the transition and removes the divergence of the correlation length. For strong enough noise ( $S \sim 10^{-5}$ ), one observes only a gradual increase of the correlation length with the density, in agreement with experiment.

We derived a model for the large-scale flows generated by ensembles of swimming bacteria. We show that the onset of coherence is attributed to the collective hydrodynamic interaction between individual objects. Our theory identifies non-trivial mechanism of typical scale selection of emergent pattern. With certain modifications, it can be applied to broader class of system, both biological [13] and inanimate [15, 16]. Our theory provides alternative approach to the description of active hydrodynamic systems (active gels) put forward in Re. [17]. We thank Michael Graham, Frank Jülicher, Karsten Kruse, Hugues Chate, and Eberhard Bodenschatz for useful discussions. This work was supported by the U.S. DOE, grants W-31-109-ENG-38.

- 
- [1] I.S. Aranson and L.S. Tsimring, Phys. Rev. E **71**, 050901(R) (2005)
  - [2] I.S. Aranson and L.S. Tsimring, cond-mat/0512659, submitted to Phys. Rev. E (2006)
  - [3] R. A. Simha and S. Ramaswamy, Phys. Rev. Lett. **89**, 058101 (2002)
  - [4] A. Sokolov, I.S. Aranson, R.E. Goldstein, and J.O. Kessler, submitted to Phys. Rev. Lett. (2006)
  - [5] X.-L. Wu and A. Libchaber, Phys. Rev. Lett. **84**, 3017 (2000)
  - [6] M. J. Kim and K. S. Breuer, Phys. Fluids **16**, L78 (2004).
  - [7] J. P. Hernandez-Ortiz, Ch. G. Stoltz, and M. D. Graham, Phys. Rev. Lett. **95**, 204501 (2005)
  - [8] C. Dombrowski, L. Cisneros, S. Chatkaew, R. E. Goldstein, and J. O. Kessler, Phys. Rev. Lett. **93**, 098103 (2004)
  - [9] N. H. Mendelson, A. Bourque, K. Wilkening, K.R. Anderson, and J.C. Watkins, J. Bacteriol. **181**, 600 (1999)
  - [10] G. Grégoire and H. Chaté, Phys. Rev. Lett. **92**, 025702 (2004)
  - [11] J. Toner and Y. Tu, Phys. Rev. Lett. **75**, 4326 (1995)
  - [12] T. Vicsek, A. Czirók, E. Ben-Jacob, I. Cohen, and O. Shochet, Phys. Rev. Lett. **75**, 1226 (1995);
  - [13] I.H. Riedel, K. Kruse, and J. Howard, Science **309** 300 (2005)
  - [14] M. Doi and S.F. Edwards, *The Theory of Polymer Dynamics*, Clarendon Press, Oxford, 1988.
  - [15] D. L. Blair, T. Neicu, and A. Kudrolli Phys. Rev. E **67**, 031303 (2003)
  - [16] I.S.Aranson and L.S.Tsimring, Phys. Rev. E **67**, 021305 (2003).
  - [17] K. Kruse et al, Phys. Rev. Lett. **92**, 078101 (2004)
  - [18] See EPAPS Document No. for animations. A direct link to this document may be found in the online article's HTML reference section. The document may also be reached via the EPAPS homepage (<http://www.aip.org/pubservs/epaps.html>) or from <ftp.aip.org> in the directory /epaps/. See the EPAPS homepage for more information.